Evidence of an Inverse Compton Origin for the HESS Spectrum of G347.3−0.5

G.E. Allen (MIT), J.C. Houck (MIT), T.G. Pannuti (Caltech), and S.J. Sturner (NASA/GSFC, USRA)

Abstract

Gamma-ray spectra of the supernova remnant G347.3−0.5 have been published by the *CANGAROO* and *HESS* collaborations. Several analyses of the *CANGAROO* data have been reported. Here we present the results of a joint spectral analysis of the *HESS* data, some *XMM* X-ray data and some *ATCA* radio data. The X-ray and radio data were fitted with a synchrotron radiation model. Inverse Compton scattering, nonthermal bremsstrahlung and neutral-pion decay models were considered for the gamma-ray data. The results of these analyses suggest that the *HESS* spectrum is dominated by inverse Compton scattered photons.

1. Introduction

The supernova remnant G347.3−0.5 is one of only a few shell-type remnants reported to emit TeV gamma rays. Both the *CANGAROO* and *HESS* collaborations report the detection of TeV gamma-ray emission from the remnant [1, 2]. While some argue that the *CANGAROO* spectrum is produced by the decay of neutral pions, an extrapolation of the π^0 spectrum to GeV energies yields a flux that is too large to be consistent with the constraints derived from *EGRET* data [3] unless only the highest energy protons diffuse far enough away from the shock to interact in high-density material [4, 5, 6]. Alternatively, the *CANGAROO* spectrum might be described by inverse Compton scattering of the cosmic microwave background radiation, but this model is incompatible with the *CANGAROO* data [4] unless the volume filled by the very-high–energy electrons is at least one hundred times larger than the volume filled by the compressed or amplified magnetic field [5, 7]. To help determine which physical process is responsible for the TeV emission from G347.3−0.5, we fitted the *HESS* spectrum with models of inverse Compton scattering, nonthermal bremsstrahlung and neutral-pion decay.

2. Data

This poster describes the results of a joint spectral analysis of some X-ray, gamma-ray and radio data for the supernova remnant G347.3−0.5. X-ray spectra for most of the remnant were obtained by analyzing data from four of five archived *XMM* observations. The fifth data set was excluded because the data are dominated by events associated with a background flare. Only data from the EPIC PN CCDs were included in the present analysis. The data were analyzed using the techniques described in the SAS Users' Guide. The fields of view of the four pointings do not span the entire extent of the supernova remnant. The fraction of the source flux in these fields was estimated using some archived *ROSAT* PSPC data. Since 71% of the total number of events associated with the source (after background subtraction) are in the four fields, the normalizations of the models used to fit the X-ray data are multiplied by a factor of 1.40 (i.e. 1/0.71).

The radio flux densities at 1.4 and 2.5 GHz (6.7±2.0 and 5.6±1.7 Jy, respectively) obtained from *ATCA* data [5] are included in the joint spectral fits. Although these results are only for the bright northwestern rim, the flux densities are assumed to represent the radio emission from the entire remnant because the emission from the feature designated as "Arc 2" in Figure 5 of [5] may not be associated with G347.3−0.5 [8].

The *HESS* spectrum was taken from Figure 3 of [2].

3. Analysis

The spectral analyses were performed using the spectral-fitting package ISIS [9] and the scripting language S-Lang [10]. The nonthermal emission spectra are based on electron and proton spectra of the form

$$\frac{dn}{dpc} = A\left(\frac{pc}{\text{GeV}}\right)^{-\Gamma} e^{(\text{GeV}-E)/\epsilon}, \qquad (1)$$

where n is the particle number density, $p = \gamma mv$, c is the speed of light, A is the number density at $p = 1$ GeV/c in units of cm^{-3} GeV^{-1}, Γ is the differential spectral index and ϵ is the exponential cut-off (or "maximum") energy. The X-ray and radio data were fitted with a synchrotron radiation model. The X-ray spectra were modified by an interstellar photoelectric absorption component. The gamma-ray data were separately fitted with inverse Compton scattering, nonthermal bremsstrahlung and neutral-pion decay models. The inverse Compton, electron-proton bremsstrahlung, electron-electron bremsstrahlung and neutral-pion decay cross sections are the ones described by [11, 12, 13, 14]. Only the cosmic microwave background radiation is used as seed photons for the inverse Compton process. The results of the fits are listed in Table 1 and shown in Figures 1–3.

Table 1: Parameters of joint fits to some *XMM*, *HESS* and *ATCA* data

Quantity	Inverse Compton	Bremsstrahlung	π^0 decay
n_H^{NW} [10^{21} cm^{-2}]	6.19 ± 0.09	6.19 ± 0.09	6.19 ± 0.09
n_H^{SW} [10^{21} cm^{-2}]	7.11 ± 0.11	7.11 ± 0.11	7.11 ± 0.11
n_H^{SE} [10^{21} cm^{-2}]	5.50 ± 0.15	5.50 ± 0.15	5.50 ± 0.15
n_H^{C} [10^{21} cm^{-2}]	3.79 ± 0.10	3.79 ± 0.10	3.79 ± 0.10
Γ	1.96 ± 0.05	1.96 ± 0.05	1.96 ± 0.05
$\epsilon^\dagger$ [TeV]	23^{+8}_{-5}	30^{+37}_{-14}	104^{+106}_{-40}
B [μG]	21^{+15}_{-9}	13^{+31}_{-10}	30
Norm$_X^{NW}$ [cm^{-2}]	$1.2^{+1.9}_{-0.7} \times 10^4$	$2.5^{+27.6}_{-2.1} \times 10^4$	6.9×10^3
Norm$_X^{SW}$ [cm^{-2}]	$8.1^{+13}_{-5.0} \times 10^3$	$1.7^{+18.4}_{-1.5} \times 10^4$	4.6×10^3
Norm$_X^{SE}$ [cm^{-2}]	$4.3^{+6.8}_{-2.6} \times 10^3$	$8.9^{+98}_{-7.6} \times 10^3$	2.5×10^3
Norm$_X^{C}$ [cm^{-2}]	$3.4^{+5.2}_{-2.1} \times 10^3$	$6.9^{+76}_{-5.9} \times 10^3$	1.9×10^3
Norm$_G$ [cm^{-2}]	$1.4^{+0.8}_{-0.6} \times 10^5$	$5.7^{+24.4}_{-2.0} \times 10^6$	5.7×10^7
Norm$_R$ [cm^{-2}]	3.9×10^4	8.0×10^4	2.2×10^4
χ^2/dof	$10190/3759$	$10190/3759$	$10190/3759$

† The cut-off energy of the electron spectrum (inverse Compton and bremsstrahlung) or proton spectrum (π^0 decay).
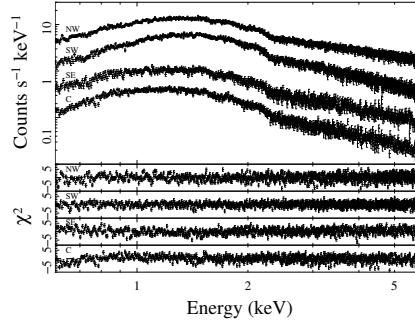

Figure 1. The *XMM* EPIC PN spectral data for the northwestern (NW), southwestern (SW), southeastern (SE) and central (C) regions of G347.3−0.5. The top panel shows, from top to bottom, the sum of the source and background spectra for the NW, SW, SE and C regions multiplied by factors of 1, 0.7, 0.2 and 0.06, respectively. Note that the scaling factor of 1.40 described in §2 is not included in the data depicted here. The last four panels show, from top to bottom, the differences between the data points and the best-fit synchrotron model divided by the uncertainties in the data points for the NW, SW, SE and C regions, respectively.
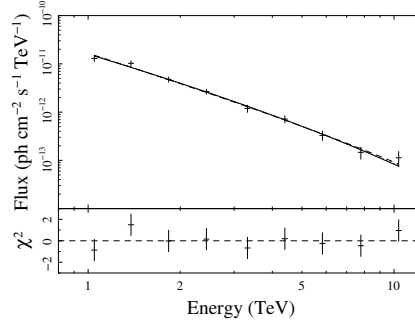

Figure 2. The *HESS* spectrum for the entire remnant G347.3−0.5 [2]. The top panel shows the source spectrum (data points) and best-fit inverse Compton scattering (solid curve), nonthermal bremsstrahlung (dashed curve) and neutral-pion decay (dotted curve) models. The bottom panel shows the differences between the data points and the inverse Compton scattering model divided by the uncertainties in the data points.
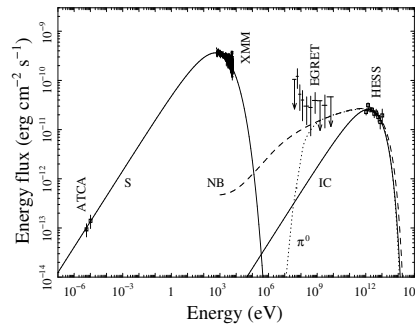

Figure 3. The radio to gamma-ray spectrum of the entire supernova remnant G347.3−0.5. The data, which are labeled vertically, include the *ATCA* results [5], the sum of the northwestern, southwestern, southeastern and central *XMM* EPIC PN spectra scaled by a factor of 1.40 (see §2), the *EGRET* spectrum [3] and the *HESS* spectrum [2]. The four curves are models of the spectra produced by synchrotron radiation (S), nonthermal bremsstrahlung (NB), the decay of neutral pions (π^0) and inverse Compton scattering of the cosmic microwave background radiation (IC).

4. Discussion

1. If the *HESS* emission is dominated by inverse Compton scattering of the cosmic microwave background radiation, then

   - The mean electron cut-off energy $\epsilon = 23^{+8}_{-5}$ TeV.
   - The mean magnetic field strength $B = 21^{+15}_{-9}$ μG.
   - The volume filled by the very-high–energy electrons is about 3.5 (1.1–11.4 at the 90% c. l.) times larger than the volume filled by the magnetic field. This result implies the *HESS* image should appear similar to the X-ray image, which is consistent with the results of [2].
   - The density $n < 40$ cm^{-3} in the volume filled by the cosmic-ray electrons. Otherwise, a significant fraction of the *HESS* flux would be produced by nonthermal bremsstrahlung. The lack of thermal X-ray emission implies $n < 0.03$ cm^{-3} [7, 15]. A high density environment ($n > 4$ cm^{-3}) would also lead to a large neutral-pion–decay flux unless the proton cut-off energy is well below 100 TeV or the high-energy proton number density is much less than one hundred times the electron number density.

2. If the *HESS* emission is dominated by nonthermal bremsstrahlung, then

   - The mean electron cut-off energy $\epsilon = 30^{+37}_{-14}$ TeV.
   - The mean magnetic field strength $B = 13^{+31}_{-10}$ μG.
   - The density $n > 40$ cm^{-3} in the region filled by the cosmic-ray electrons. Otherwise, a significant fraction of the *HESS* flux would be produced by inverse Compton scattering. A density this high may be incompatible with the lack of thermal X-ray emission and suggests that the *HESS* image should be similar to the CO image to the extent that the CO emission traces the matter density. However, the *HESS* image [2] is inconsistent with the CO image [16]. A high density environment would also lead to a significant neutral-pion–decay flux unless the proton cut-off energy is well below 100 TeV or the high-energy proton number density is less than ten times the electron number density.

3. If the *HESS* emission is dominated by the decay of neutral pions, then

   - The mean proton cut-off energy $\epsilon = 104^{+106}_{-40}$ TeV (which is below the "knee" at 3000 TeV).
   - The density $n > 4$ cm^{-3} in the region filled by the cosmic-ray protons. Otherwise, a significant fraction of the *HESS* flux would be produced by inverse Compton scattering. Again, a high density may be incompatible with the lack of evidence of thermal X-ray emission and suggests that the *HESS* image should be similar to the CO image, which does not seem to be the case.

5. Conclusions

The *HESS* spectrum is well fitted by an inverse Compton model. The inverse Compton normalization is about 3.5 times larger than the synchrotron normalization, which suggests that the very-high–energy electrons fill a volume about three times larger than the volume filled by the magnetic field. This result suggests that the *HESS* image should be similar to the X-ray image, which is consistent with the results of [2]. Since the volume ratio is expected to be greater than one, inverse Compton scattering must play a significant, if not dominant, role in the production of the TeV emission from G347.3−0.5. If the *HESS* spectrum is dominated by inverse Compton scattering, then the ambient density must be small. Otherwise, the nonthermal bremsstrahlung and neutral-pion decay spectra would be important. The lack of evidence of thermal X-ray emission indicates the ambient density is quite low ($n < 0.03$ cm^{-3}). Therefore, the *HESS* spectrum and image and the low ambient density can be easily understood if the TeV emission is dominated by inverse Compton scattering. However, if the TeV emission is dominated by either nonthermal bremsstrahlung or the decay of neutral pions, then it is difficult to understand the similarities between the *HESS* and X-ray images, the lack of similarities between the *HESS* and CO images and the lack of thermal X-ray emission. For these reasons, we believe that the *HESS* spectrum is dominated by inverse Compton scattering of the cosmic microwave background radiation.

References

[1] H. Muraishi et al., Astron. Astrophys. 354, L57 (2000). R. Enomoto et al., Nature. 416, 823 (2002).
[2] F. A. Aharonian et al., Nature. 432, 75 (2004).
[3] O. Reimer, O. and M. Pohl, Astron. Astrophys. 390, L43 (2002).
[4] Y. Uchiyama et al., Astron. Astrophys. 400, 567 (2003).
[5] J. S. Lazendic et al., Astrophys. J. 602, 271 (2004).
[6] M. A. Malkov et al., Astrophys. J. in press (2005).
[7] T. G. Pannuti et al., Astrophys. J. 593, 377 (2003).
[8] D. C. Ellison et al., Astrophys. J. 563, 191 (2001).
[9] J. C. Houck and L. A. DeNicola, Astronomical Data Analysis Software and Systems IX (2000), ASP Conf. Ser. 216, ed. N. Manset, C. Veillet, & D. Crabtree, (San Francisco: ASP), 591. http://space.mit.edu/ASC/ISIS/.
[10] http://www.jedsoft.org/slang/.
[11] O. Klein and Y. Nishina, Z. Phys., 52, 853 (1929).
[12] W. Heitler, The Quantum Theory of Radiation, 3rd ed., New York: Dover (1953).
[13] E. Haug, Z. Naturforsch., 30a, 1099 (1975).
[14] F. A. Aharonian and A. M. Atoyan, Astron. Astrophys., 362, 937 (2000).
[15] G. Cassam-Chenaï et al., Astron. Astrophys. 427, 199 (2004).
[16] Y. Fukui et al., Publ. Astron. Soc. Jpn. 55, L61 (2003).